IJRCS

International Journal of Robotics and Control Systems
Vol. 5, No. 4, 2025, pp. 2360-2378
ISSN 2775-2658
http://pubs2.ascee.org/index.php/ijrcs

ASCEE

Optimized Speed Regulation of BLDC Motors: A Comparative Performance Study of Artificial Neural Networks and Super-Twisting Sliding Mode Controllers

Anwar Hasni [a,1,*], Hassan El Fadil [a,2], Abdellah Lassioui [a,3], Marouane El Ancary [a,4], Yassine El Asri [a,5], Ahmed. Hamed [a,6], Sidina EL Jeilani [a,7]

[a] ISA Laboratory, National School of Applied Sciences (ENSA), Ibn Tofail University, Kénitra 14000, Morocco
[1] hasni.anwar20@gmail.com; [2] elfadilhassan@yahoo.fr; [3] abdellah.lassioui@uit.ac.ma; [4] marouane.elancary@gmail.com; [5] elasriyassine@yahoo.com; [6] ahmedmohamed.hamed@uit.ac.ma; [7] sidinamedahid@gmail.com
* Corresponding Author

ARTICLE INFO

Article history
Received July 28, 2025
Revised September 16, 2025
Accepted November 14, 2025

Keywords
Artificial Intelligence;
BLDC Motor;
ANN Controller;
STSMC Controller;
Speed Control

ABSTRACT

Brushless DC (BLDC) motors have seen substantial development across a wide range of applications, driven by their high performance and inherent robustness. As a result, the demand for accurate control of speed and torque has grown considerably. Despite numerous control strategies from traditional PID controllers to more recent artificial intelligence-based methods achieving precise speed control for BLDC motors remains a significant challenge. This article explores the enhancement of BLDC motor speed control through a comparative analysis of two advanced control strategies: an Artificial Neural Network (ANN) controller, representing intelligent control methods from the field of artificial intelligence, and a Super-Twisting Sliding Mode Controller (STSMC), recognized for its strong robustness against external disturbances. The originality of this work lies in studying systematically the trade-off between control quality and computational complexity for both ANN and STSMC. The simulation results obtained using Matlab/Simulink demonstrate and validate the performance of both controllers. The tests are generally conducted under two scenarios. In the first scenario, the motor is subjected to a constant load torque; the results show that the ANN controller has a response time of 0.25 seconds, while the STSMC is faster with a response time of 0.17 seconds. In the second scenario, under a load torque disturbance, the response times are 0.42 seconds for the ANN and 0.15 seconds for the STSMC.

1. Introduction

The development of brushless direct current (BLDC) motors is a significant advancement over traditional brushed motors, a cleaner high-performance technology. Brushed motors have a number of inherent disadvantages, such as frictional loss, increased noise and needs for regular maintenance due to brush and commutator wear [1]. These disadvantages have prompted ongoing research into more reliable, longer-lasting and energy-efficient motor technologies. BLDC motors solve these problems by eliminating wear-susceptible mechanical components such as brushes and commutators.

Instead, they use electronic commutation, which is usually regulated by an inverter and powered through Hall sensors or sensorless methods [2]. This concept lowers power consumption, increases power densities, increases working times and improves overall efficiency [3]. It is because of these reasons that BLDC motors are increasingly being used today in a number of applications such as high-performance, reliability and durability.

Increasing technology creates the demand for brushless DC motors in various industries such as automotive, aerospace, robotics and precision manufacturing [4]. BLDC motors have a few major advantages over induction motors: faster dynamic response, improved resolution torque control and improved energy efficiency. But these advantages are trailed by some disadvantages, i.e., high initial cost and sophisticated control systems [5]. Even though BLDC motors are physically identical to Permanent Magnet Synchronous Motors (PMSM), both utilize different commutation techniques. BLDC motors utilize rectangular (trapezoidal) commutation, while PMSM motors use sinusoidal commutation [6].This significant difference puts BLDC motors in a premium when quick starting, rapid gear shifting or delicate dynamic response is required [7].

An operation of a BLDC motor relies on an electronic inverter that switches current through stator windings, offering a replacement for brushes and commutator used in traditional DC motors. The commutation is synchronized with the rotor's angular position, normally sensed by Hall-effect sensors [8]. These sensors offer instantaneous information essential to inverter control and smooth, accurate motor rotation maintenance [9]. In more advanced systems, however, physical sensors can be eliminated altogether with sensorless control algorithms. These techniques estimate the position of the rotor from analyzing motor voltage and current signals [10], [11].

BLDC motor control and power supply techniques are categorized into several classes depending on whether position sensors and power converters are used [12]. Sensor-based techniques, that is, using Hall-effect sensors or optical encoders, enable accurate sensing of rotor position with maximum commutation and efficient torque control at low speed. However, they add to the cost, system size, and environmental sensitivity [13]. Sensorless techniques employ estimation algorithms that obtain rotor position from motor terminal voltages or currents. While they reduce hardware complexity and cost, they are less accurate at low speed, and therefore their application in systems requiring high accuracy is still low [14]. Moreover, power converter control, generally founded on a three-phase inverter, allows accurate speed and torque control by methods like Pulse Width Modulation (PWM), Field-Oriented Control (FOC), or six-step commutation [15]. Conversely, low-cost or constant-speed applications will sometimes use control without converters through basic switching circuits, usually at the cost of energy efficiency and dynamic response [16]. Therefore, the choice of control strategy strongly depends on cost constraints, precision requirements, efficiency targets, and the specific application domain [17], [18].

In the literature, several methods of control have been suggested. The most common is the classical PID (Proportional–Integral–Derivative) controller as it is simple to implement and cheap [19]. For adjusting its parameters under the influence of disturbances, various empirical methods are commonly employed, such as the Ziegler-Nichols method (via step response or ultimate gain) [20], the Cohen-Coon method [21], and the Tyreus-Luyben method [22], all aimed at striking a balance among speed of response, stability, and ease of implementation. At a more analytical level, approaches such as pole placement, H∞ optimization, and frequency analysis (Bode and Nyquist diagrams) enable the design of high-performance PID controllers based on mathematical models of the system [23]. In addition, numerical optimization techniques and artificial intelligence methods provide powerful alternatives for tuning controllers in nonlinear or complex systems [24]. Among these are evolutionary algorithms such as PSO (Particle Swarm Optimization) [25], GA (Genetic Algorithm) [26], and GWO (Grey Wolf Optimizer) [27]. These are complemented by machine learning approaches, including neural networks, adaptive fuzzy logic, and direct search methods like the Nelder-Mead method or gradient descent [28], [29].

Fuzzy logic control is also widely used owing to its ability to handle uncertainty and load fluctuation without a precise mathematical model of the motor [30]. Model Predictive

Control (MPC) is a mature technique that predicts future system dynamics so that dynamic constraints can be handled efficiently at the cost of increased computational complexity [31]. Moreover, Sliding Mode Control (SMC) [32], and more specifically its enhanced version called Super-Twisting SMC [33], is highly regarded due to its robustness to uncertainties and because it allows for exact tracking even in the presence of disturbances [34], [35].

With the emergence of artificial intelligence approaches, there have been new intelligent controllers, especially those based on neural networks and reinforcement learning algorithms, that can adjust control actions adaptively in response to actual operating conditions [36]. The selection of the control strategy or algorithm is therefore a trade-off between performance, robustness, computational complexity, and simplicity of implementation, depending on the application [37], [38].

The cruise control of the BLDC motor remains one of the top challenges and a primary focus of current research. The most important contribution of this paper is presenting a new control method based on two extremely advanced controllers: an Artificial Neural Network and a Super-Twisting Sliding Mode Controller. The paper provides a thorough comparison of these two methods in terms of response time, stability, and robustness based on the analysis of various operating conditions and perturbed cases. The approach provides more accurate estimation of the dynamic performance and flexibility of each method, thus introducing new areas of intelligent and robust control of BLDC motors.

Despite these numerous approaches, most existing studies have focused either on conventional control techniques or on isolated intelligent methods, without providing a systematic comparison of robustness against stochastic load variations and sensorless operation. Recent work on sensorless control of BLDC motors [39], [40] highlights the growing need for reliable controllers capable of maintaining high accuracy even in the absence of position sensors, particularly at low speeds. However, there remains a lack of research on the evaluation of the behavior of advanced controllers, such as artificial neural networks and super-twisting sliding mode control, in the presence of unpredictable disturbances and estimation uncertainties. This gap motivates the present study, where we hypothesize that the intrinsic chattering reduction offered by STSMC can improve stability and robustness, while ANNs provide adaptive learning capabilities for better dynamic performance.

The study presented in this article is structured in a clear and logical manner. Following an introduction that provides the context of the subject, outlines the research problem, reviews the existing literature, and presents the proposed contribution, the second section addresses the mathematical modeling of the BLDC motor. The third section is devoted to the presentation of the two controllers used, detailing their respective operating principles. The fourth section presents the simulation results, along with a comprehensive comparison of the obtained performances and a critical discussion of the findings. Finally, the article concludes with a summary of the work conducted and offers perspectives for future research directions in the field of intelligent control of BLDC motors.

2. BLDC Motor Modeling

This part will try to provide the mathematical model of the BLDC motor model, divided into two fundamental parts. The first section will be in charge of the analysis of the equivalent circuit diagram, electric and mechanical equations of the BLDC motor. The second section will deal with the analysis of the transfer function considering two working modes: no-load and loaded.

2.1. BLDC motor dynamics modeling

Mathematical model of the two pairs of poles BLDC three-phase motor is discussed in this first subsection, according to its electrical and mechanical equations [41]. The stator consists of a full-pitch winding in Y (star) connection, whereas the rotor features a smooth surface polar structure. Three Hall-effect sensors are symmetrically positioned with a 120-degree electrical offset, ensuring precise and balanced commutation [42], [43]. Furthermore, the mathematical equations describing the

behavior of the BLDC motor are derived based on a set of simplifying assumptions, which are detailed below.

- Disregarding cardiac saturation, eddy currents and deceleration.
- Remove the armature feedback and observe the magnetic field spreading from the air gap as a trapezoidal wave with a smooth top spanning 120 electrical angles.
- Ignore the effect of feedback and assume that electrically conductive elements are distributed uniformly and continuously over the surface of the armature.
- The control circuit switches and handwheel diodes in the power inverter circuit provide perfect switching performance.

Equivalent schematic of the BLDC drive shown in Fig. 1.

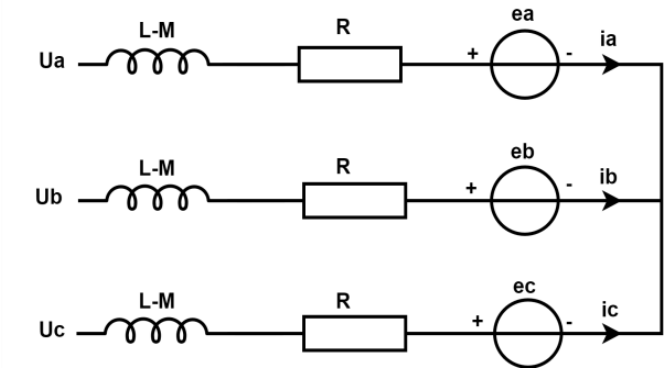

Fig. 1. Brushless motor equivalent diagram

Single-phase electrical equation for a BLDC motor can be expressed as:

$$v_a = R \cdot i_a + L \cdot \frac{di_a}{dt} + e_a \tag{1}$$

Phase voltage equation in matrix form for a three-phase BLDC motor is:

$$\begin{bmatrix} v_a \\ v_b \\ v_c \end{bmatrix} = R \begin{bmatrix} i_a \\ i_b \\ i_c \end{bmatrix} + L \frac{d}{dt} \begin{bmatrix} i_a \\ i_b \\ i_c \end{bmatrix} + \begin{bmatrix} e_a \\ e_b \\ e_c \end{bmatrix} \tag{2}$$

Phase voltage equation based on line voltage can be derived as:

$$v_{ab} = v_a - v_b = R(i_a - i_b) + L \frac{d(i_a - i_b)}{dt} + (e_a - e_b) \tag{3}$$

Instantaneous electromagnetic power transferred to the rotor is given by:

$$P_{em} = e_a i_a + e_b i_b + e_c i_c \tag{4}$$

Represents the useful power (excluding losses), directly linked to torque production. Assuming no mechanical or parasitic losses:

$$P_{em} = T_e \cdot \Omega \tag{5}$$

The electromagnetic torque can be expressed as:

$$T_e = \frac{3}{2} \cdot P \cdot K_t \cdot \psi \cdot \sin(\theta) \tag{6}$$

Or, in general:

$$T_e = \frac{3}{2} \cdot P \cdot (e_a i_a + e_b i_b + e_c i_c)/\Omega \quad (7)$$

The dynamic equation describing rotor motion is:

$$T_e - T_r = J \cdot \frac{d\Omega}{dt} + B \cdot \Omega \quad (8)$$

2.2. Transfer function of the BLDC motor

The transfer function constitutes a fundamental structured model in control system theory. It provides a simplified representation of a system's dynamic behavior, and the mathematical models derived from it are widely used in various fields of automatic control. Several analysis and design methods, such as pole placement and frequency feedback techniques, have been developed based on this classical approach rooted in transfer function theory [44], [45]. In this context, the transfer function of a BLDC motor plays a key role in performance analysis and control system design. Unlike conventional DC motors, BLDC motor windings are energized as a function of the rotor position, and are typically configured in three-phase or multi-phase arrangements. However, the fundamental principles governing the electromotive force (EMF) and electromagnetic torque generation per phase are similar to those in standard brushless DC drives, making it possible to adopt analogous analysis approaches [46], [47].

Let us examine the scenario in which a three-phase BLDC inverter operates under full-bridge control in two-phase conduction mode. In this mode, at any given instant, two of the three stator windings are energized while the third remains inactive. For example, when phase A and phase B are conducting, the current conditions can be defined as:

$$\begin{cases} i_a = -i_b = i \\ \dfrac{di_a}{dt} = -\dfrac{di_b}{dt} = \dfrac{di}{dt} \end{cases} \quad (9)$$

Under these conditions, the line voltage U_{ab} can be reformulated as:

$$U_{ab} = 2R \cdot i + 2(L - M) \cdot \frac{di}{dt} + 2K_e \cdot \Omega \quad (10)$$

Formula (10) expresses the voltage loop equation of the printed circuit precisely when the two-phase windings are energized, with the corresponding equivalent circuit shown in Figure 1. It's worth mentioning that the same circuit shown in Fig. 2 can also be used in the three-phase half-bridge and three-phase full-bridge drive types of the BLDC motor, taking into account the specific values of Ke and Kt.

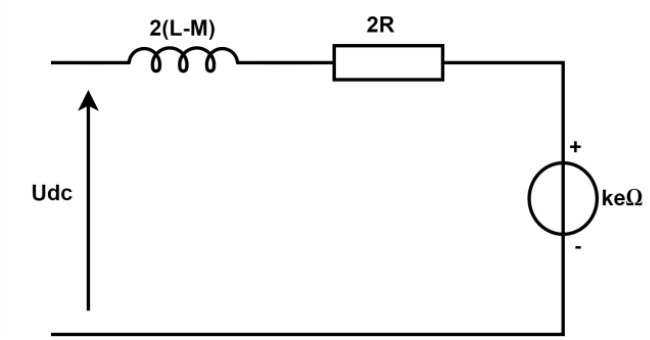

Fig. 2. Equivalent two-phase BLDC motor circuit.

Initially, when the BLDC motor operates under no-load conditions, the current can be expressed in terms of the angular speed as:

$$i(t) = \frac{J}{K_t} \cdot \frac{d\Omega(t)}{dt} \tag{11}$$

By substituting this expression into the line voltage equation, we obtain a new differential equation that relates the DC input voltage to the motor's angular velocity:

$$U_d(t) = r_a \cdot \left(\frac{J}{K_t} \cdot \frac{d\Omega(t)}{dt}\right) + L_a \cdot \frac{d}{dt}\left(\frac{J}{K_t} \cdot \frac{d\Omega(t)}{dt}\right) + K_e \cdot \Omega(t) \tag{12}$$

Applying the Laplace transform to this time-domain equation yields the no-load transfer function of the BLDC motor, which links the Laplace-transformed angular speed $\Omega(s)$ to the input voltage $U_d(s)$:

$$\frac{\Omega(s)}{U_d(s)} = \frac{1}{K_e + \frac{r_a J}{K_t} s + \frac{L_a J}{K_t} s^2} \tag{13}$$

When a load torque T_r is applied, the mechanical equation must also be considered:

$$T_e - T_r = J \cdot \frac{d\Omega}{dt} + B \cdot \Omega \tag{14}$$

Combining the electrical and mechanical models and transforming into the Laplace domain, the complete transfer function for the system becomes:

$$\Omega(s) = \frac{U_d(s)}{K_e + \frac{r_a J}{K_t} s + \frac{L_a J}{K_t} s^2 + \frac{B}{K_t} s} - \frac{T_r(s)}{Js + B} \tag{15}$$

3. Controller Design

This section aims to present the operating principle and structure of the two controllers analyzed in this article: the artificial neural network and the super-twisting sliding mode controller. It is organized into two complementary subsections. The first is dedicated to the ANN controller, detailing its architecture, training phase, and the performance achieved after training. The second subsection focuses on the STSMC controller, highlighting its operating principle, structural design, and the underlying mathematical model. In this study, the originality lies in the joint optimization of the PID and STSMC controller parameters to ensure the quality of the data used for training the artificial neural network and to guarantee a fair comparison between the two control strategies. In practice, the PID parameters, used to generate input-output data for the ANN, as well as the STSMC gains K1 and K2, were adjusted offline using the Grey Wolf Optimizer (GWO) algorithm [48].

3.1. Artificial Neural Network Controller

Artificial Neural Networks are inspired by the operating principles of the human nervous system. They are built upon a mathematical model composed of interconnected neurons, organized according to well-defined relationships in order to accomplish a specific task [49]. The system is structured around three main layers: the input layer, the hidden layer, and the output layer [50]. Control is achieved by transferring external information and data from the input layer to the output layer through activation functions [51]. This feature enables the ANN to conform to different system scenarios, whether linear or non-linear, so that the system perfectly reproduces the desired response.

In this study, an artificial neural network is developed using data collected from a PID controller, with the goal of training the model and assessing its ability to respond to the dynamic behavior of a BLDC motor [52], [53]. The neural network has two neurons distributed in two layers. The input to it is the error signal, i.e., the difference between the desired mechanical speed and the actual speed of the motor. The network outputs the appropriate supply voltage that must be provided in order to achieve the desired speed. The artificial neural network is trained using data from the PID controller, which is taken as a reference to enhance the robustness and agility of the control system. The Fig. 3 illustrates the artificial neural network block diagram used in this research, its structure, and operation principle [54], [55].

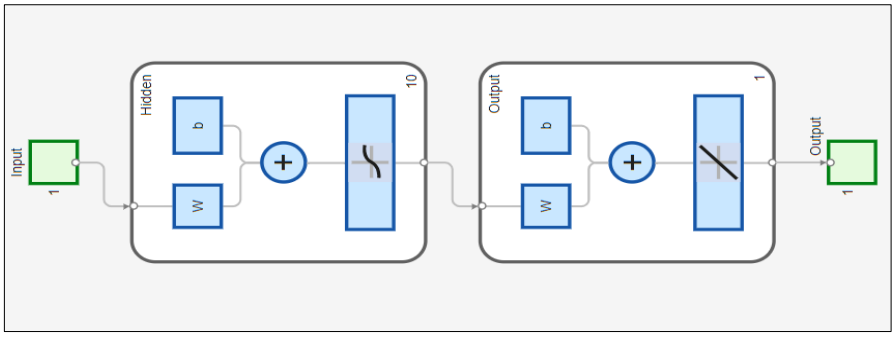

Fig. 3. The perceptron concept is the neural artificial perception model chosen.

The behavior of an artificial neural network can be described by the following equations:

$$y_k = \sum_{k=1}^{n} w_k^{(2)} \cdot g\left(\sum_{j=1}^{p} w_{kj}^{(1)} \cdot \Phi_j + b_k^{(1)}\right) + b^{(2)} \tag{16}$$

The activation function, selected here as a sigmoid function, is defined as follows:

$$g(x) = \frac{2}{1 + e^{-x}} - 1 \tag{17}$$

This structure confers on the network the ability to approximate dynamic non-linear relationships by modifying weights and biases during learning.

Fig. 4 show the simulation scheme used for closed-loop control of a brushless motor with a controller based on an artificial neural network. This model was developed following the collection of data from a traditional speed control loop based on a PID controller. The system receives a desired speed setpoint, which is then compared with the actual motor speed to generate an error signal. This error is fed into the neural network, which produces a control signal in the form of a voltage. The neural network is designed to handle the system's non-linearities and uncertainties, based on a mathematical model of the motors dynamic performance. The schematic highlights the adaptive capabilities of the ANN controller, which learns the system dynamics in real time, enabling robust, precise, non-linear speed control.

Fig. 5 presents an analysis of the results of an artificial neural network applied to the modeling or control of a brushless DC motor system. It is divided into four sub-figures, each offering a particular analysis of the results obtained.

(a) Network Performance Curve:

This subset highlights the evolution of the root mean square error (RMSE) throughout the learning process, clearly underlining the convergence of the model and its effectiveness in reducing error on the training, validation and test datasets.

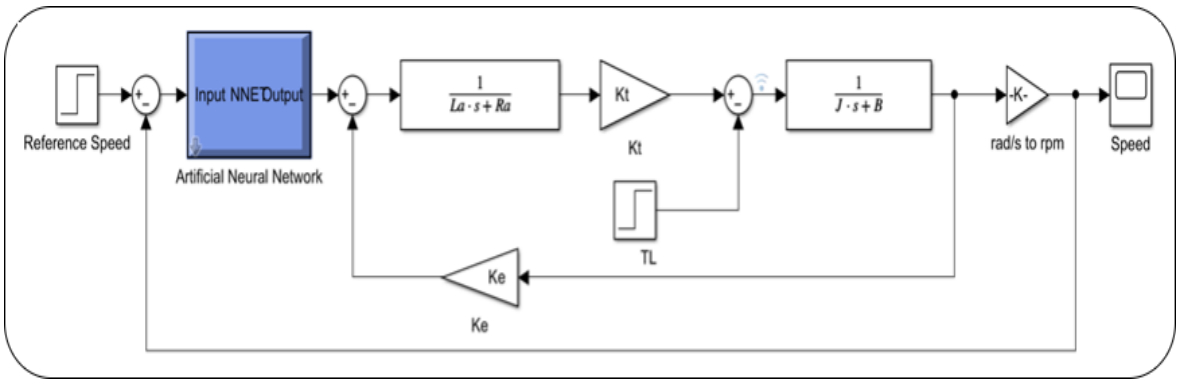

Fig. 4. Control architecture of a brushless DC motor using an ANN

(b) Optimization and Stopping Criteria:

Key learning parameters such as the gradient, learning rate (μ) and validation process are highlighted in this profile, underlining both the effectiveness and robustness of the training, as well as the systematic early-stop process put in place to avoid over-fitting.

(c) Prediction Error Histogram:

This subplot displays the distribution of prediction errors across all data points. The strong concentration around zero underscores the model's accuracy and its minimal deviation from the expected results.

(d) Network Output Fit to Reference Values:

This plot compares the predicted outputs to the reference values, showing a close match and low residual errors. It highlights the model's ability to accurately learn and reproduce the underlying functional relationship.

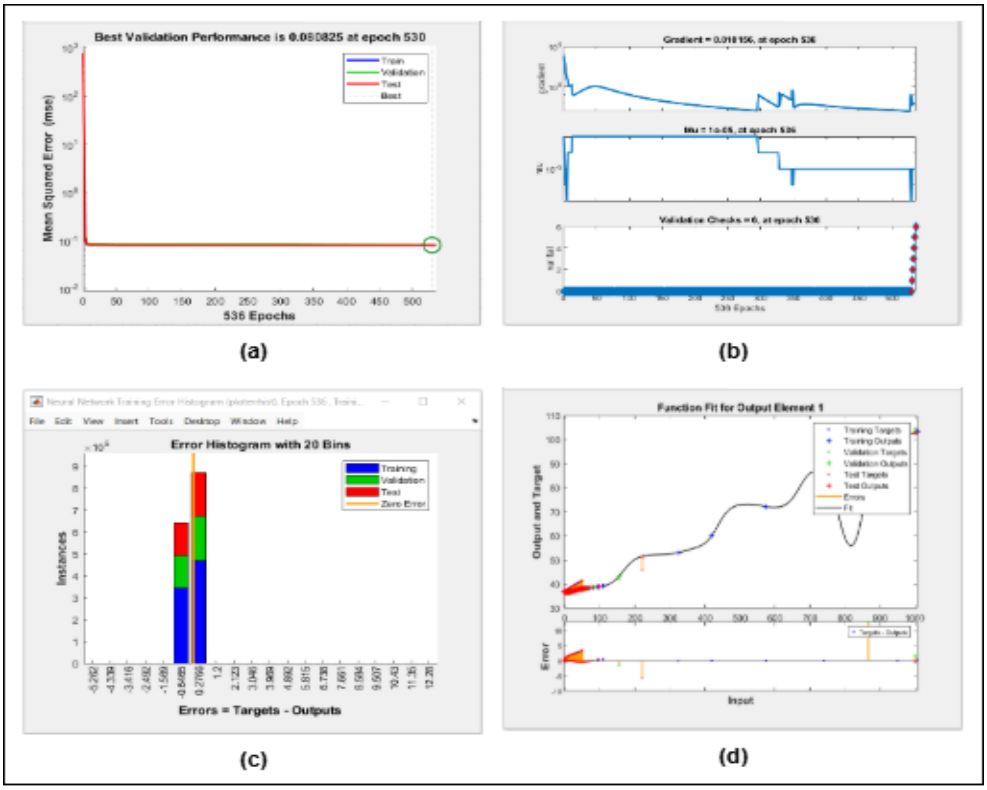

Fig. 5. Comprehensive performance evaluation; (a) Network performance curve, (b) Optimization parameters and stopping criteria, (c) Histogram of prediction errors, (d) Adjustment of network outputs to targets.

3.2. Second-Order Sliding Mode Controller

This section is dedicated to the development of the second controller investigated in this study: the Super-Twisting Sliding Mode Controller [56]. The aim is to conduct a comparative analysis between this controller and the previously developed Artificial Neural Network controller, using performance criteria such as speed tracking accuracy for the BLDC motor and robustness against load variations. The adopted strategy is based on STSMC, which utilizes the error between the desired speed and the actual motor speed to generate a control signal in the form of voltage. This control voltage is applied to the motor model to ensure that the motor follows the desired speed, as illustrated in Fig. 6.

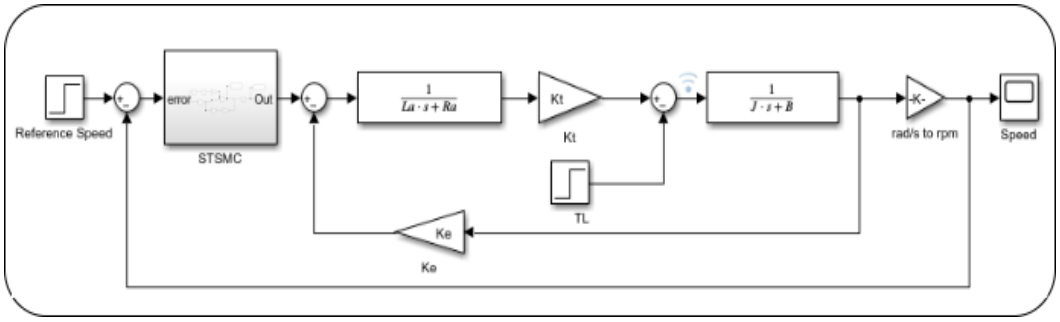

Fig. 6. Control architecture of a brushless DC motor using STSMC controller

The primary objective is to ensure that the motor speed V_{motor} accurately tracks the user-defined reference speed V_{ref} [57]. To achieve this, the following sliding surface is defined:

$$S = V_{\text{motor}} - V_{\text{ref}} \tag{18}$$

While the conventional Sliding Mode Controller (SMC) aims to bring the system state to the surface defined by $S = 0$, the Super-Twisting Sliding Mode Controller (SOSMC) seeks to satisfy both $S = 0$ and $\dot{S} = 0$, thereby enhancing robustness and response speed [58]. To reduce the chattering effect caused by disturbances and model uncertainties, the Super-Twisting Sliding Mode Control technique is employed [59], [60]. The corresponding control law is given by:

$$V_{\text{cmd}} = -K_1\sqrt{|S|}\,\text{sign}(S) - K_2\int_0^t \text{sign}\,(S)\,d\tau \tag{19}$$

This technique enables more accurate and extensive control, high reference tracking accuracy and robustness against external disturbances of the BLDC motor load torque.

4. Results and Discussion

This section is dedicated to presenting the simulation results obtained using the Matlab/Simulink environment, based on the two controllers employed in this study. The first is an artificial neural network controller, while the second is based on the Super-Twisting sliding mode control technique. The objective is to evaluate the performance of each controller and compare them in terms of stability, response speed, tracking accuracy, and resistance to load torque disturbances. The two scenarios speed tracking and robustness against disturbances enable an effective assessment of each control strategy under various operating conditions, while also highlighting their respective strengths and limitations. A detailed analysis was carried out to better understand the dynamic behaviors observed, taking into account the sophisticated characteristics specific to each controller. In conclusion, a comparative evaluation grid was developed based on criteria such as tracking performance, response time, and adaptability to external disturbances, with the aim of identifying the most efficient and suitable solution for the intended control objectives. Table 1 summarizes the various parameters used in this study and during the simulations.

Table 1. Parameters used in the different simulation scenarios

Designation	Value
V_{DC}	300 V
R	1.5 Ω
L	0.0115 H
M	0.005 H
K_t	0.0603
K_e	0.0603
J	0.001 Kg.m^2
B	0.002 N.m

4.1. First scenario: tracking performances

The evaluation of the results is carried out through two scenarios: tracking performance and controller robustness. This section is dedicated to comparing the first scenario between the Artificial Neural Network controller and the Super-Twisting Sliding Mode Controller. Fig. 7 illustrates the motor speed response for both controllers: the blue curve corresponds to the ANN, while the red curve represents the STSMC. The ANN controller reaches the desired speed after 0.25 s with no overshoot, whereas the STSMC reaches the setpoint in 0.17 s with a slight overshoot. Regarding the tracking error, the difference between the reference speed and the measured speed, it vanishes after 0.25 s for the ANN and 0.17 s for the STSMC, as shown in Fig. 8.

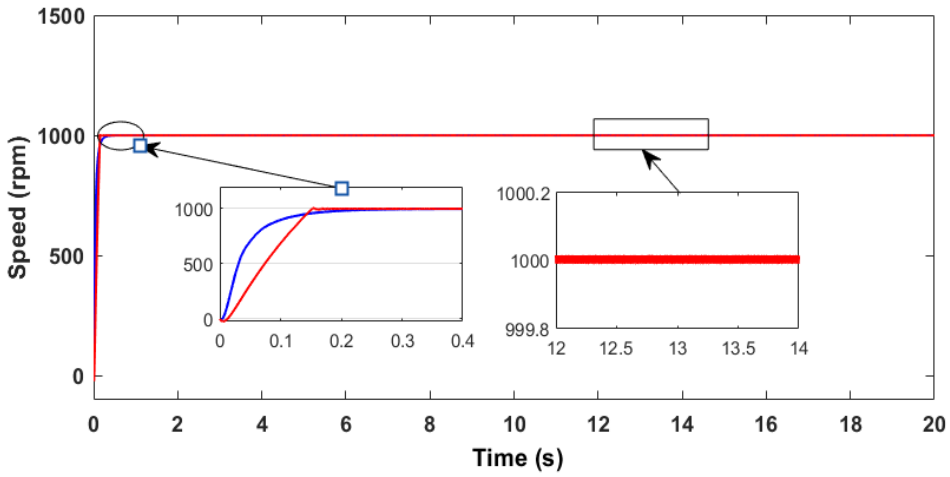

Fig. 7. The motor speed response to a constant speed reference.

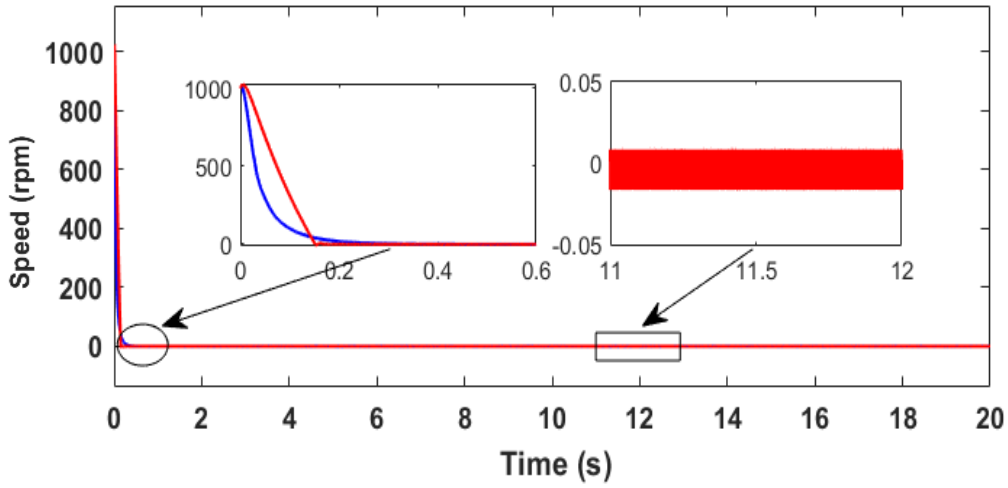

Fig. 8. Speed tracking error with constant reference speed.

Fig. 9 presents the output voltage of the controllers. For the ANN, the voltage saturates at 40 V to supply the BLDC motor and reach 1000 rpm. In contrast, the output of the STSMC shows frequency variations around 1.53 kHz, oscillating between 0 V and 50 V. To evaluate the ability to follow a variable reference, Fig. 10 shows the motor response to a speed change from 800 rpm to 1000 rpm. The response time after this variation is 0.35 s for the ANN with 2% ripple, compared to 0.05 s for the STSMC with only 0.5% ripple. Fig. 11 illustrates the tracking error after the speed variation. It vanishes after 0.2 s for the ANN and 0.07 s for the STSMC, with the same peak error amplitude of approximately 200 rpm for both controllers. Fig. 12 shows the controller output voltage during the speed change: 42 V for the ANN, and a constant 50 V with no variation for the STSMC. All these tracking performance measurements were carried out under a fixed load torque of 1N.m, as shown in Fig. 13.

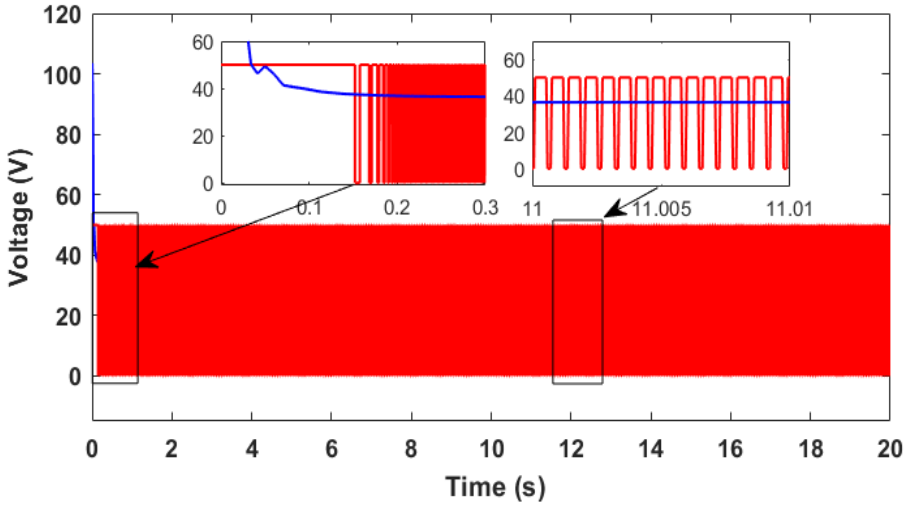

Fig. 9. Controllers output voltage with constant speed reference.

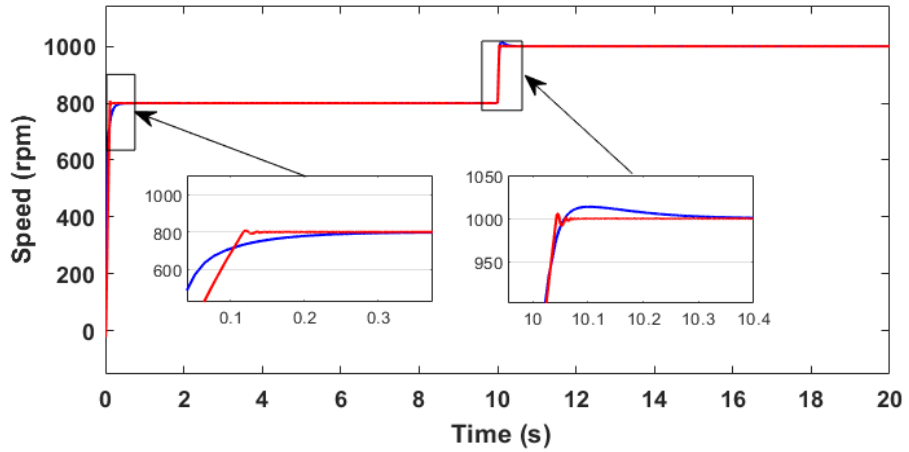

Fig. 10. Motor speed variation during change in reference speed with load condition fixe.

4.2. Second scenario: robustness performances

Regarding the second scenario, it aims to assess the robustness of both controllers in the face of load torque disturbances. Fig. 14 shows the motor speed response during a sudden change in load torque. For the ANN controller, recovery after the disturbance occurs within 0.42 s, with a peak ripple of approximately 200 rpm, representing 20% of the reference value. In comparison, the STSMC controller stabilizes in just 0.15 s, with a reduced ripple of 50 rpm, or 5%, demonstrating superior dynamic stability. Regarding the tracking error, it quickly vanishes after the disturbance, as illustrated in Fig. 15 confirming both controllers' ability to restore the setpoint. Fig. 16 displays the controller

output voltages during the application of a variable torque load. For the ANN, the voltage ranges from 40 V to 45 V, whereas the STSMC output oscillates between 0 V and 65 V, then stabilizes at 65 V precisely at the moment of the torque variation. This robustness test was carried out under a load torque variation from 1 N.m to 2 N.m, as shown in Fig. 17.

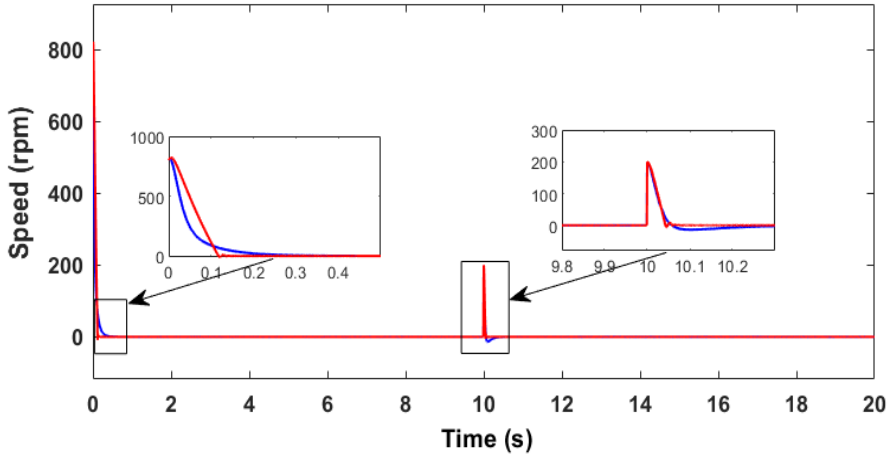

Fig. 11. Speed tracking error with variable reference speed.

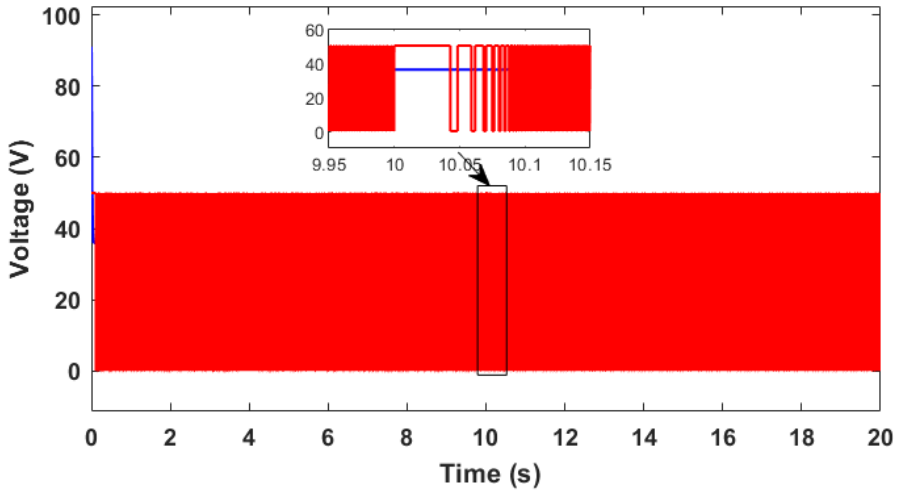

Fig. 12. Controllers output voltage with variable speed reference.

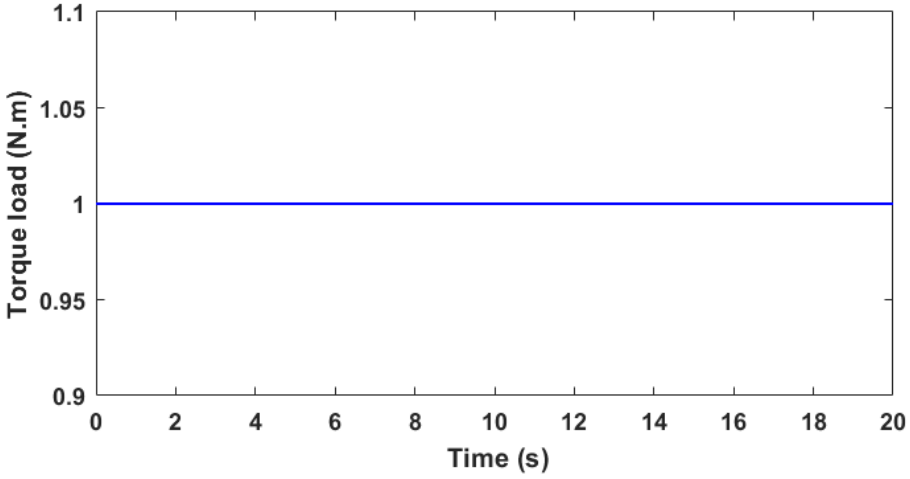

Fig. 13. Load condition applied to the motor.

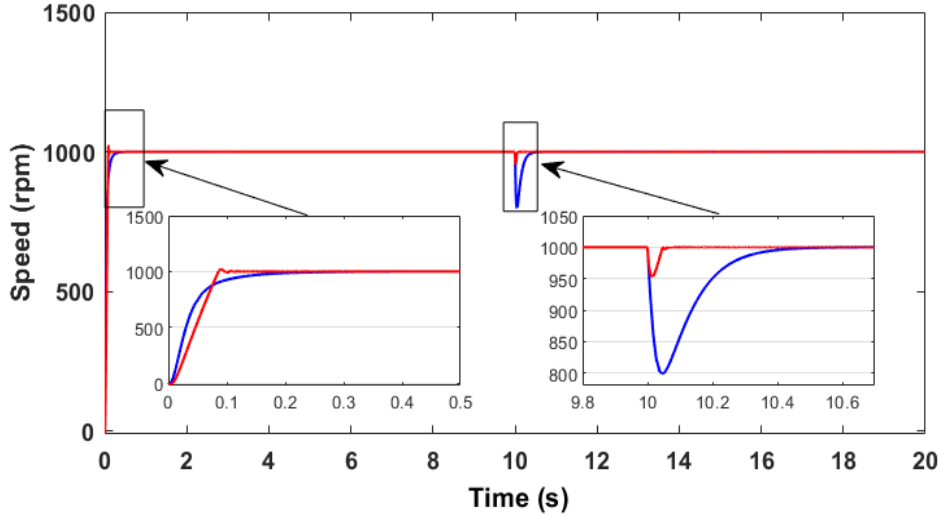

Fig. 14. Motor speed response to load torque variation.

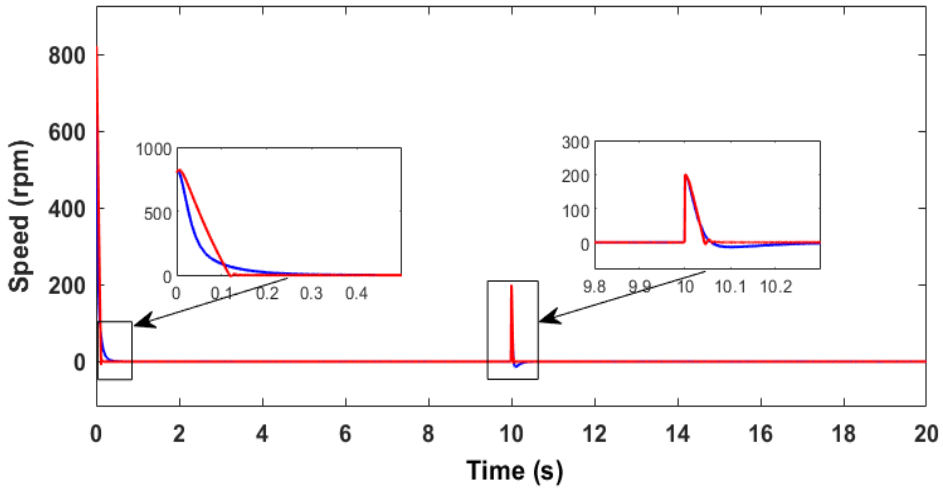

Fig. 15. The speed error during change in load torque.

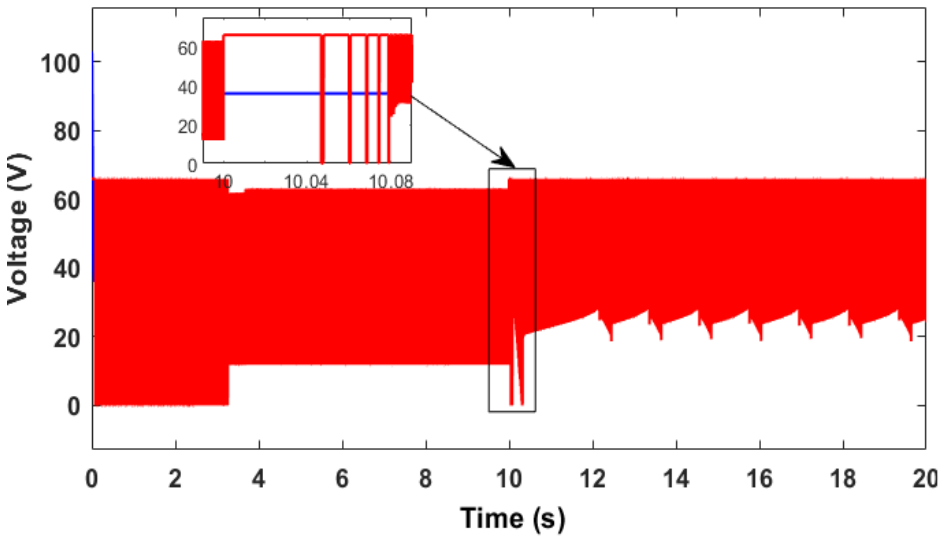

Fig. 16. The controller output voltage during change in the load torque.

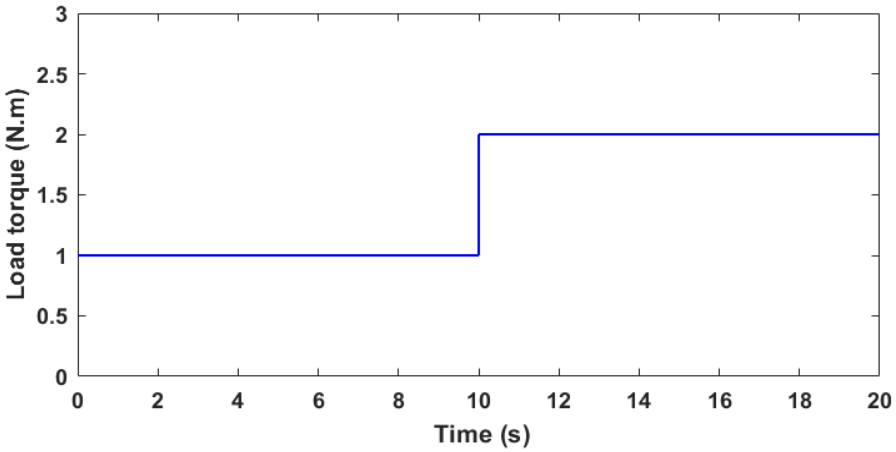

Fig. 17. Increasing load condition applied to the motor

4.3. Figures and Tables

As a summary of this study and the simulation results obtained, it can be concluded that both controllers demonstrate noteworthy performance, each with its own specific advantages. The ANN controller shows promising results thanks to training based on data from an optimized PID controller, allowing for accurate speed tracking. However, its performance remains sensitive to the quality of the training data, and it has limitations when dealing with load torque disturbances. Additionally, the execution time of the algorithms depends heavily on the performance of the processors and hardware used. On the other hand, the STSMC controller exhibits very strong results in terms of reaction speed, response accuracy, and robustness against load disturbances. Nonetheless, it is important to acknowledge that tuning the controller parameters optimally can be a challenging task, which may affect its overall performance. The comparative results, in terms of response time, response ripple, and disturbance recovery time, as well as the two main evaluation criteria: speed tracking and robustness, are summarized in Table 2.

Table 2. Summary of comparison results

Controller	Response Time	Disturbance Recovery Time	Ripple During Torque Disturbance	Speed Tracking Performance	Robustness
ANN	0.25s	0.42s	15%	High	High
STSMC	0.17s	0.15s	20%	High	Excellent

5. Conclusion

This study proposed a comparative analysis between a controller based on an artificial neural network, trained from an optimized PID, and a super-twisted sliding mode controller applied to the speed control of a BLDC motor. Simulation results showed that STSMC offers greater robustness against disturbances and load variations, while ANN provides satisfactory dynamic response with relatively low implementation complexity. This complementarity suggests that the choice of the most appropriate controller depends on the operating conditions: the STSMC is more suitable for highly disturbed environments, and the ANN is suitable for applications requiring fast response and a simple control structure. Beyond these results, this study highlights the importance of optimizing the parameters of both controllers using the Grey Wolf Optimizer algorithm, which ensured a fair comparison and significantly improved their respective performances. However, certain limitations must be acknowledged. First, the validations were carried out solely by simulation, without practical experimentation on a test bench, which limits the scope of the conclusions in terms of real applicability. Second, the ANN used remains relatively simple in architecture and is trained offline using PID data, without explicitly taking into account parametric uncertainties or measurement noise.

As such, its “adaptive” nature must be qualified, since it is a static predictive model rather than an online learning model. These findings nevertheless open up concrete research prospects that are consistent with the results obtained. These include extending this methodology to more advanced or hybrid ANN architectures (ANN–STSMC) in order to combine robustness and intelligence, the integration of reinforcement learning techniques to enable adaptive real-time adjustment, and experimental validation on a hardware platform to assess the practical constraints related to computational load, sensor limitations, and real-time stability. These future developments build directly on the foundations laid by this work and will enable progress towards more reliable control strategies that are better suited to industrial applications.

Author Contribution: All authors contributed equally to the main contributor to this paper. All authors read and approved the final paper.

Acknowledgment: This work was carried out with the support of the Centre National de la Recherche Scientifique et Technique (CNRST), as part of the "PhD-Associate Scholarship - PASS" program.

Conflicts of Interest: The authors declare no conflict of interest.

Nomenclatures:

v_a, v_b, v_c - Phase voltages (V)
R - Phase resistance (Ω)
L - Self-inductance (H)
i_a, i_b, i_c - Phase currents(A)
e_a, e_b, e_c - Phase back-EMFs (V)
T_e - Electromagnetic torque (Nm)
Ω - Angular speed (rad/s)
P - Number of pole pairs
K_t - Torque constant (Nm/A)
ψ - Maximum permanent magnet flux linkage (Wb)
θ - Rotor position (electrical rad)
T_r - Load torque (Nm)
J - Moment of inertia (kg·m²)
B - Viscous friction coefficient (N·m·s)
U_{dc} - DC bus voltage (V)
$r_a = 2R$ - Equivalent line resistance (Ω)
$L_a = 2(L - M)$ - Equivalent line inductance (H)
K_e - Back-EMF constant (V.s/rad)
i - Line current (A)
Ω - Angular speed (rad/s)
Φ_j - represents the input to the network
$w_{kj}^{(1)}$, $b_k^{(1)}$ - are the weights and biases of the hidden layer
$g(x)$ - is the activation function.

References

[1] J. Sundaram and K. R., “A new wedge shaped inner rotor for a BLDC motor: Performance analysis,” *Thermal* Science *and Engineering Progress*, vol. 54, p. 102863, Sept. 2024, https://doi.org/10.1016/j.tsep.2024.102863.

[2] P. Leninpugalhanthi and R. Latha, "Adaptive PID controller based direct torque control of fuel cell fed BLDC drive for industrial drives applications," *Thermal Science and Engineering Progress*, vol. 55, p. 102931, Oct. 2024, https://doi.org/10.1016/j.tsep.2024.102931.

[3] J.-C. Gamazo-Real, V. Martínez-Martínez, and J. Gomez-Gil, "ANN-based position and speed sensorless estimation for BLDC motors," *Measurement*, vol. 188, p. 110602, Jan. 2022, https://doi.org/10.1016/j.measurement.2021.110602.

[4] R. Arivalahan, S. Venkatesh, and T. Vinoth, "An effective speed regulation of brushless DC motor using hybrid approach," *Advances in Engineering Software*, vol. 174, p. 103321, Dec. 2022, https://doi.org/10.1016/j.advengsoft.2022.103321.

[5] S. S. A. Naqvi *et al.*, "Multi-objective optimization of PI controller for BLDC motor speed control and energy saving in Electric Vehicles: A constrained swarm-based approach," *Energy Reports*, vol. 12, pp. 402–417, Dec. 2024, https://doi.org/10.1016/j.egyr.2024.06.019.

[6] M. Jalanko, Y. Sanchez, V. Mahalec, and P. Mhaskar, "Adaptive system identification of industrial ethylene splitter: A comparison of subspace identification and artificial neural networks," *Computers & Chemical Engineering*, vol. 147, p. 107240, Apr. 2021, https://doi.org/10.1016/j.compchemeng.2021.107240.

[7] R. G. and D. V., "Artificial neural network controller based cleaner battery-less fuel cell vehicle with EF2 resonant DC-DC converter," *Sustainable Computing: Informatics and Systems*, vol. 35, p. 100667, Sept. 2022, https://doi.org/10.1016/j.suscom.2022.100667.

[8] F. D. John Lionel, J. Jayan, M. K. Srinivasan, and P. Prabhakaran, "DC-link current based position estimation and speed sensorless control of a BLDC motor used for electric vehicle applications," *International Journal of Emerging Electric Power Systems*, vol. 22, no. 3, pp. 269–284, June 2021, https://doi.org/10.1515/ijeeps-2020-0235.

[9] A. Sikora, A. Zielonka, M. Woźniak, P. Orság, T. Mlčák, and L. Hrabovský, "Fuzzy control system to improve the efficiency of the brushless direct current motor by correcting the control angle," *International Journal of Electrical Power & Energy Systems*, vol. 169, p. 110762, Aug. 2025, https://doi.org/10.1016/j.ijepes.2025.110762.

[10] N. Hemalatha, S. Venkatesan, R. Kannan, S. Kannan, A. Bhuvanesh, and A. S. Kamaraja, "Sensorless speed and position control of permanent magnet BLDC motor using particle swarm optimization and ANFIS," *Measurement: Sensors*, vol. 31, p. 100960, Feb. 2024, https://doi.org/10.1016/j.measen.2023.100960.

[11] C. O. Omeje and A. O. Salau, "Torque ripples enhancement of a PMBLDC motor propelled through quadratic DC–DC boost converter at varying load," *ISA Transactions*, vol. 143, pp. 385–397, Dec. 2023, https://doi.org/10.1016/j.isatra.2023.08.027.

[12] Z. B. Abdullah, S. W. Shneen, and H. S. Dakheel, "Performance enhancement of BLDC motor drive systems using fuzzy logic control and PID controller for improved transient response and stability," *International Journal of Robotics and Control Systems*, vol. 5, no. 2, pp. 1552–1570, June 2025, https://doi.org/10.31763/ijrcs.v5i2.1882.

[13] A. Hasni, H. El Fadil, A. Lassioui, A. Intidam, M. El Ancary, Y. El Asri, and S. Nady, "Reinforcement learning-based control strategy for BLDC motors," *J. Eur. Systèmes Autom.*, vol. 58, no. 6, pp. 1111–1121, Jun. 2025, https://doi.org/10.18280/jesa.580603.

[14] M. Dasari, A. Srinivasula Reddy, and M. Vijaya Kumar, "A comparative analysis of converters performance using various control techniques to minimize the torque ripple in BLDC drive system," *Sustainable Computing: Informatics and Systems*, vol. 33, p. 100648, Jan. 2022, https://doi.org/10.1016/j.suscom.2021.100648.

[15] A. Bamimore, A. B. Osinuga, T. E. Kehinde-Abajo, A. S. Osunleke, and O. Taiwo, "A comparison of two artificial neural networks for modelling and predictive control of a cascaded three-tank system," *IFAC-PapersOnLine*, vol. 54, no. 21, pp. 145–150, Jan. 2021, https://doi.org/10.1016/j.ifacol.2021.12.025.

[16] A. Modi, N. Joshi, and A. Mehta, "Robust discrete-time super twisting formation protocol for a 6-DOF quadcopter swarm," *ISA Transactions*, vol. 143, pp. 177–187, Dec. 2023, https://doi.org/10.1016/j.isatra.2023.09.029.

[17] M. Divandari, B. Rezaie, and A. Ranjbar Noei, "Speed control of switched reluctance motor via fuzzy fast terminal sliding-mode control," *Computers & Electrical Engineering*, vol. 80, p. 106472, Dec. 2019, https://doi.org/10.1016/j.compeleceng.2019.106472.

[18] M. W. Hasan, A. S. Mohammed, and S. F. Noaman, "An adaptive neuro-fuzzy with nonlinear PID controller design for electric vehicles," *IFAC Journal of Systems and Control*, vol. 27, p. 100238, Mar. 2024, https://doi.org/10.1016/j.ifacsc.2023.100238.

[19] A. D. M. Africa, J. O. Q. Chua, and J. L. H. Solis, "PID tuning of speed controller using Ziegler–Nichols and manual method DC motor," in *Proc. 2023 IEEE 15th Int. Conf. Humanoid, Nanotechnology, Information Technology, Communication and Control, Environment, and Management (HNICEM)*, Nov. 2023, pp. 1–6, https://doi.org/10.1109/HNICEM60674.2023.10589041.

[20] R. Firmansyah and R. Irmawanto, "Comparison study of PI controller tuning method to regulate the DC motor speed," in *Proc. 2021 3rd Int. Conf. Research and Academic Community Services (ICRACOS)*, Oct. 2021, pp. 93–97, https://doi.org/10.1109/ICRACOS53680.2021.9702007.

[21] B. N. Kommula and V. R. Kota, "Design of MFA-PSO based fractional order PID controller for effective torque controlled BLDC motor," *Sustain. Energy Technol. Assess.*, vol. 49, p. 101644, Feb. 2022, https://doi.org/10.1016/j.seta.2021.101644.

[22] R. Baz, K. El Majdoub, F. Giri, and O. Ammari, "Fine-tuning quarter vehicle performance: PSO-optimized fuzzy PID controller for in-wheel BLDC motor systems," *IFAC-Pap.*, vol. 58, no. 13, pp. 715–720, Jan. 2024, https://doi.org/10.1016/j.ifacol.2024.07.566.

[23] P. M. Preethiraj and J. B. Edward, "Design of novel DC-DC interleaved boost converter for BLDC application," *Heliyon*, vol. 10, no. 22, p. e40041, Nov. 2024, https://doi.org/10.1016/j.heliyon.2024.e40041.

[24] D. Potnuru, K. A. Mary, and Ch. S. Babu, "Experimental implementation of flower pollination algorithm for speed controller of a BLDC motor," *Ain Shams Eng. J.*, vol. 10, no. 2, pp. 287–295, Jun. 2019, https://doi.org/10.1016/j.asej.2018.07.005.

[25] L. Yang, C. Qu, B. Jia, and S. Qu, "The design of an affordable fault-tolerant control system of the brushless DC motor for an active waist exoskeleton," *Neural Comput. Appl.*, vol. 35, no. 3, pp. 2027–2037, Jan. 2023, https://doi.org/10.1007/s00521-022-07362-7.

[26] J. E. MuraliDhar and P. Varanasi, "A progressive rugged appearance of fuzzy controller fed four-switch BLDC drive," *Procedia Comput. Sci.*, vol. 47, pp. 144–152, Jan. 2015, https://doi.org/10.1016/j.procs.2015.03.193.

[27] R. Baz, K. E. Majdoub, F. Giri, and A. Taouni, "Self-tuning fuzzy PID speed controller for quarter electric vehicle driven by in-wheel BLDC motor and Pacejka's tire model," *IFAC-Pap.*, vol. 55, no. 12, pp. 598–603, Jan. 2022, https://doi.org/10.1016/j.ifacol.2022.07.377.

[28] K. M. A. Prasad, A. Unnikrishnan, and U. Nair, "Fuzzy sliding mode control of a switched reluctance motor," *Procedia Technol.*, vol. 25, pp. 735–742, Jan. 2016, https://doi.org/10.1016/j.protcy.2016.08.167.

[29] N. L. Guo, P. Ge, D. Sun, and Y. Qiao, "Adaptive cruise control based on model predictive control with constraints softening," *Appl. Sci.*, vol. 10, no. 5, Art. no. 51635, Jan. 2020, https://doi.org/10.3390/app10051635.

[30] P. N., R. Thirumalaivasan, and B. Ashok, "Design of sliding mode controller with improved reaching law through self-learning strategy to mitigate the torque ripple in BLDC motor for electric vehicles," *Comput. Electr. Eng.*, vol. 118, p. 109438, Sept. 2024, https://doi.org/10.1016/j.compeleceng.2024.109438.

[31] S. Ullah, R. Hayat, K. Zeb, A. Rasheed, and S. M. Muyeen, "Super-twisting sliding mode controller for energy storage system of a novel multisource hybrid electric vehicle: Simulation and hardware validation," *Int. J. Hydrog. Energy*, vol. 71, pp. 952–963, Jun. 2024, https://doi.org/10.1016/j.ijhydene.2024.05.326.

[32] G. V. Hollweg, P. J. D. de O. Evald, D. M. C. Milbradt, R. V. Tambara, and H. A. Gründling, "Design of continuous-time model reference adaptive and super-twisting sliding mode controller," *Math. Comput. Simul.*, vol. 201, pp. 215–238, Nov. 2022, https://doi.org/10.1016/j.matcom.2022.05.014.

[33] A. Goswami, M. Sreejeth, and M. Singh, "Analysis and Mitigation of Hall Sensor Glitch Effects in Brushless DC Motor Based E-Vehicle Controller," in *Signals, Machines and Automation (SIGMA 2022)*, A. Rani, B. Kumar, V. Shrivastava, and R. C. Bansal, Eds., Lecture Notes in Electrical Engineering, vol. 1023. Singapore: Springer, 2023, pp. 89–98, https://doi.org/10.1007/978-981-99-0969-8_8.

[34] H. Chen, Q. Li, S. Tang, N. Aït-Ahmed, J. Han, T. Wang, Z. Zhou, T. Tang, and M. Benbouzid, "Adaptive super-twisting control of doubly salient permanent magnet generator for tidal stream turbine," *International Journal of Electrical Power & Energy Systems*, vol. 128, p. 106772, 2021, https://doi.org/10.1016/j.ijepes.2021.106772.

[35] M. Sall, A. Kebe, I. Gueye, and M. Diop, "Comparative study between the PID regulator and the fuzzy regulator applied to the operation of a brushless DC motor," *Energy Power Eng.*, vol. 13, no. 11, pp. 365–376, Nov. 2021, https://doi.org/10.4236/epe.2021.1311025.

[36] A. F. Al-Saoudi, K. M. Al-Aubidy, and A. J. Al-Mahasneh, "Comparison of PID, Fuzzy Logic, ANFIS and Model Predictive Controllers for Cruise Control System," in *Proc. 2024 21st Int. Multi-Conf. Syst., Signals & Devices (SSD)*, Apr. 2024, pp. 263–265, pp. 263–265, https://doi.org/10.1109/SSD61670.2024.10548200.

[37] L. Luque-Vega, B. Castillo-Toledo, and A. G. Loukianov, "Robust block second order sliding mode control for a quadrotor," *J. Frankl. Inst.*, vol. 349, no. 2, pp. 719–739, Mar. 2012, https://doi.org/10.1016/j.jfranklin.2011.10.017.

[38] E. Natsheh, "Enhancing field-controlled DC motors with artificial intelligence-infused fuzzy logic controller," *J. Appl. Data Sci.*, vol. 6, no. 1, pp. 455–469, 2025, https://doi.org/10.47738/jads.v6i1.508.

[39] T. T. Sarkar and C. Mahanta, "Gain tuned sliding mode control based maximum power point tracking for solar PV systems," *IFAC-Pap.*, vol. 55, no. 1, pp. 417–422, Jan. 2022, https://doi.org/10.1016/j.ifacol.2022.04.069.

[40] M. S. Hasan, A. F. Sharaf, M. D. Albakhait, and A. I. Jaber, "High performance rectifier/multilevel inverter based BLDC motor drive with PI controller," *IOP Conf. Ser. Mater. Sci. Eng.*, vol. 745, no. 1, p. 012005, Feb. 2020, https://doi.org/10.1088/1757-899X/745/1/012005.

[41] K. Xia, Y. Ye, J. Ni, Y. Wang, and P. Xu, "Model predictive control method of torque ripple reduction for BLDC motor," *IEEE Trans. Magn.*, vol. 56, no. 1, pp. 1–6, Jan. 2020, https://doi.org/10.1109/TMAG.2019.2950953.

[42] M. El-Sefy, A. Yosri, W. El-Dakhakhni, S. Nagasaki, and L. Wiebe, "Artificial neural network for predicting nuclear power plant dynamic behaviors," *Nucl. Eng. Technol.*, vol. 53, no. 10, pp. 3275–3285, Oct. 2021, https://doi.org/10.1016/j.net.2021.05.003.

[43] Y. I. M. A. Mashhadany, A. K. Abbas, and S. S. Algburi, "Modeling and analysis of brushless DC motor system based on intelligent controllers," *Bull. Electr. Eng. Inform.*, vol. 11, no. 6, pp. 2995–3003, Dec. 2022, https://doi.org/10.11591/eei.v11i6.4365.

[44] S. A. Aessa, S. W. Shneen, and M. K. Oudah, "Optimizing PID controller for large-scale MIMO systems using flower pollination algorithm," *J. Robot. Control (JRC)*, vol. 6, no. 2, pp. 553–559, Mar. 2025, https://doi.org/10.18196/jrc.v6i2.24409.

[45] U. Ishwarya, R. Srimathi, K. Nithishkumar, K. R. M. Vijaya Chandrakala, S. Saravanan, and V. K. Arun Shankar, "Optimum speed control of permanent magnet synchronous motor using artificial neural network-based field-oriented controller," in *Proc. 3rd Int. Conf. Artif. Intell. Internet Things (AIIoT)*, May 2024, pp. 1–6, https://doi.org/10.1109/AIIoT58432.2024.10574751.

[46] H. S. Dakheel, Z. B. Abdullah, N. S. Jasim, and S. W. Shneen, "Simulation model of ANN and PID controller for direct current servo motor by using MATLAB/Simulink," *TELKOMNIKA Telecommun. Comput. Electron. Control*, vol. 20, no. 4, pp. 922–932, Aug. 2022, https://doi.org/10.12928/telkomnika.v20i4.23248.

[47] R. Ristiana, S. Kaleg, A. C. Budiman, S. Sudirja, A. Hapid, A. Muharam, and Amin, "Novel hybrid-MPCC approach to generate switching sequence for six-step commutation of BLDC motor using Hall effect sensor," *Alexandria Engineering Journal*, vol. 82, pp. 43–54, 2023, https://doi.org/10.1016/j.aej.2023.09.052.

[48] S. Usha, P. M. Dubey, R. Ramya, and M. V. Suganyadevi, "Performance enhancement of BLDC motor using PID controller," *Int. J. Power Electron. Drive Syst. (IJPEDS)*, vol. 12, no. 3, pp. 1335–1344, Sept. 2021, https://doi.org/10.11591/ijpeds.v12.i3.pp1335-1344.

[49] A. Mamadapur and G. Unde Mahadev, "Speed control of BLDC motor using neural network controller and PID controller," in *Proc. 2nd Int. Conf. Power Embedded Drive Control (ICPEDC)*, Aug. 2019, pp. 146–151, https://doi.org/10.1109/ICPEDC47771.2019.9036695.

[50] M. Jabari and A. Rad, "Optimization of speed control and reduction of torque ripple in switched reluctance motors using metaheuristic algorithms based PID and FOPID controllers at the edge," *Tsinghua Sci. Technol.*, vol. 30, no. 4, pp. 1526–1538, Aug. 2025, https://doi.org/10.26599/TST.2024.9010021.

[51] X. Zhang and H. Lin, "Fault diagnosis and compensation strategy of BLDC motor drives with Hall sensors," *Xibei Gongye Daxue Xuebao (J. Northwest. Polytech. Univ.)*, vol. 37, pp. 1278–1284, Dec. 2019, https://doi.org/10.1051/jnwpu/20193761278.

[52] F. F. Ahmad, C. Ghenai, A. K. Hamid, and M. Bettayeb, "Application of sliding mode control for maximum power point tracking of solar photovoltaic systems: A comprehensive review," *Annu. Rev. Control*, vol. 49, pp. 173–196, Jan. 2020, https://doi.org/10.1016/j.arcontrol.2020.04.011.

[53] R. G. and D. V., "Artificial neural network controller based cleaner battery-less fuel cell vehicle with EF2 resonant DC–DC converter," *Sustain. Comput. Inform. Syst.*, vol. 35, p. 100667, Sept. 2022, https://doi.org/10.1016/j.suscom.2022.100667.

[54] A. Hasni, A. Lassioui, H. El Fadil, Y. El Asri, M. El Ancary, I. Bentalhik, S. El Jeilani, and S. Nady, "Cruise control of an electric vehicle propelled by a BLDC motor," *EPJ Web of Conferences*, vol. 330, art. 06008, 2025, https://doi.org/10.1051/epjconf/202533006008.

[55] A. Sikora, A. Zielonka, M. Woźniak, P. Orság, T. Mlčák, and L. Hrabovský, "Fuzzy control system to improve the efficiency of the brushless direct current motor by correcting the control angle," *Int. J. Electr. Power Energy Syst.*, vol. 169, p. 110762, Aug. 2025, https://doi.org/10.1016/j.ijepes.2025.110762.

[56] A. Hasni, H. El Fadil, A. Lassioui, M. El Ancary, Y. El Asri, H. Abbade, A. Fhail, and S. El Meslouhi, "Integrated adaptive cruise control and BLDC motor drive for optimal speed regulation in electric vehicles," in *Proc. 2025 Int. Conf. on Circuit, Systems and Communication (ICCSC)*, 2025, pp. 1–6, https://doi.org/10.1109/ICCSC66714.2025.11135306.

[57] X. Yao, C. Ma, J. Zhao, and F. De Belie, "Rapid estimation and compensation method of commutation error caused by Hall sensor installation error for BLDC motors," *IET Electr. Power Appl.*, vol. 14, no. 3, pp. 337–347, Mar. 2020, https://doi.org/10.1049/iet-epa.2018.5941.

[58] Z. B. Abdullah, S. W. Shneen, and H. S. Dakheel, "Performance enhancement of BLDC motor drive systems using fuzzy logic control and PID controller for improved transient response and stability," *Int. J. Robot. Control Syst.*, vol. 5, no. 2, pp. 1552–1570, June 2025, https://doi.org/10.31763/ijrcs.v5i2.1882.

[59] A. Hasni, A. Lassioui, H. El Fadil, M. El Ancary, Y. El Asri, S. Nady, A. Fhail, H. Abbade, and M. Chiheb, "A comprehensive review of advanced control strategies of adaptive cruise control system in electric vehicles," in *Proc. 2025 5th Int. Conf. on Innovative Research in Applied Science, Engineering and Technology (IRASET)*, 2025, pp. 1–7, https://doi.org/10.1109/IRASET64571.2025.11008174.

[60] S. N. Rao, B. M. K. Kumar, B. M. Manjunatha, and A. S. Kumar, "Modified invasive weed optimization MPPT approach for PV system interfaced with BLDC motor for water pumping system," *Journal of Engineering and Applied Science*, vol. 72, no. 1, p. 78, 2025, https://doi.org/10.1186/s44147-025-00651-7.